Electronic Supplementary Material (ESI) for Lab on a Chip

Supplementary Information

Ratcheted Electrophoresis for Rapid Particle Transport

Aaron M. Drews, Hee-Young Lee, Kyle J.M. Bishop

1. Transport of dissolved species
2. Experimental details and velocity measurements
3. Construction of barriers for the particle separator
4. Down-channel velocity reduction
5. Movie details

1. Transport of dissolved species

As noted in the main text, the motion of aqueous agarose beads in the ratcheted channel was identical to that of the silver-coated hollow glass spheres. Fig. S1 shows a series of images of the directed motion of a 36 μm agarose bead (V_o = 800 V, L = 140 μm) similar to the series shown in Fig. 1 of the main text; the dyed beads appear black because high-speed image acquisition was monochromatic.

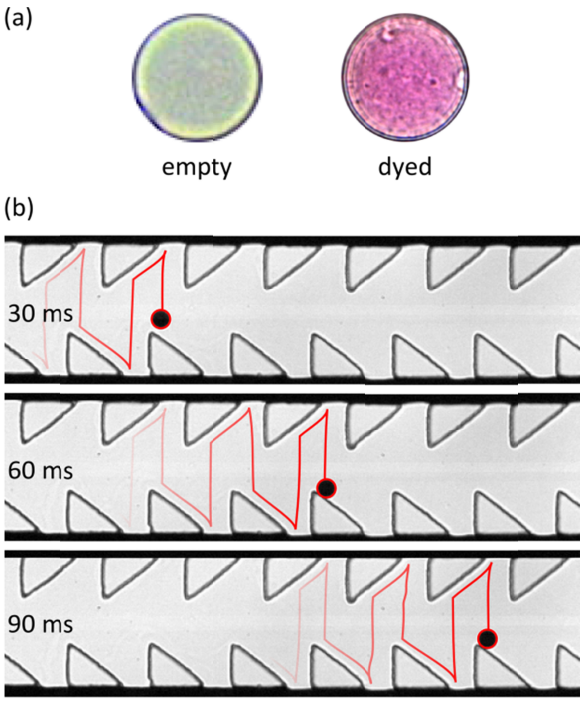

Figure S1 (a) Optical images of empty and dyed agarose beads. **(b)** Reconstructed particle trajectories show the directed motion of a 36 μm dyed agarose bead. The distance between the two electrodes was L = 140 μm; the applied voltage was V_o = 800 V.

An aqueous suspension of agarose beads was obtained from Sigma Aldrich (S6657 Superdex 75, 22-44 μm) and used without further purification. To load beads with dye, 100 μL

of the agarose suspension and five drops of red food coloring were added to 5 mL of deionized water and mixed for five minutes to allow for dye penetration. The dyed beads were separated from the water by filter paper, collected via spatula, and quickly transferred to 5 mL of mineral oil; the oil-bead mixture was sonicated for 10 minutes before use.

2. Experimental details and velocity measurements

Fabrication: Microfluidic devices were fabricated via soft lithography[1]. Polydimethysiloxane monoliths (PDMS, Sylgard 184; dielectric constant, $\varepsilon \approx 2.2$) were cast from photolithographically patterned wafers and adhered to glass substrates by UV treatment. Wide channels (~500 μm) were patterned to facilitate injection of liquid gallium (at ~40 ^{o}C) to form inherently aligned electrodes which were then frozen into place at room temperature[2]. Channels for oil and particle suspensions were ~150 μm wide. The PDMS teeth were spaced with openings of ~40 μm between teeth – large enough to allow particle contact with the electrodes but small enough to prevent the liquid gallium from flowing into the center channel during the electrode injection process.

Operation: In a typical experiment, a conductive particle (silver-coated hollow glass sphere, Cospheric M18) of diameter D = 10-20 μm was immersed in a dielectric liquid (mineral oil, Sigma Aldrich M5904; dielectric constant, $\varepsilon = 2.5$; viscosity, $\eta = 0.027$ Pa·s) and flowed into the PDMS devices describe above and shown in Fig. 1c. Application of a DC voltage V_o (Trek 20/20C controlled via Keithley 2612A) across the electrodes caused the particle to oscillate parallel to the applied field with a portion of its motion biased by the teeth in a direction perpendicular to the field (Fig. 1d). For particle velocity measurements, fluid flow was stopped for five minutes prior to application of the electric field; in other instances (Fig. 2b and Fig. 3 in the main text) flow was maintained by a syringe pump. For tracer studies, 1 μm polystyrene spheres (Polysciences 19518) were dispersed in mineral oil by sonication for 30 min before use. We tracked the position of particles (and tracers) in time using an optical microscope and a high speed camera. Using reconstructed particle trajectories, we measured the particle velocity along

the directions parallel and perpendicular to the electric field as a function of its magnitude, $E_o = V_o / L$.

Velocity measurement: Particle velocity parallel and perpendicular to the field (*i.e.*, cross-channel and down-channel velocities) were reported in the main text in Fig. 2a; the process for obtaining these values is detailed here. Each high-speed movie was converted from its proprietary format (12-bit cine) to a standard format (8-bit AVI) and the (x, y) particle location in every frame was determined via particle tracking in MATLAB[3]; particle traces were constructed from these data (Fig. S1b and Fig. 1d, 2b and 3c,d in the main text). To determine the cross-channel velocity (parallel to the field), we performed linear regression on each cross-channel segment of the particle trace resulting in n = 5-10 individual velocities for each experiment (Fig. S2b shows 12 velocities u_i). The cross-channel velocity of the particle was calculated as the mean of these individual velocities ($u = n^{-1}\Sigma u_i$). This process was repeated for several particles at the same field strength; the resulting cross-channel velocities (scaled by the particle diameter) u / D were averaged and this value reported. The reported error represents the standard deviation of these replicates.

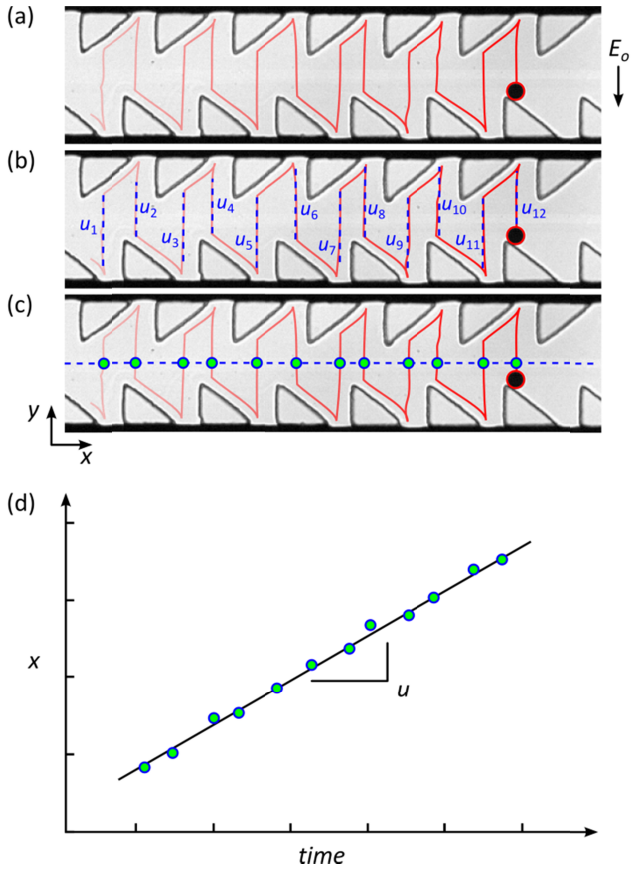

Fig. S2 *Velocity measurements*. **(a)** Particle position data were extracted from movies using standard particle tracking algorithms. **(b)** Cross-channel velocity was reported as the mean of several measurements (typically, 5-10 with 12 values shown here), each of which were determined by linear regression of the *y*-component of the particle location during a cross-channel transit. **(c)** Time and *x*-location of the particle when it crossed the channel centerline were recorded; linear regression of these points as in **(d)** was used to determine the down-channel velocity and its error was reported as the 95% confidence interval on the regression coefficient. For both velocities, normalized u / D values were averaged if several points were available at the same field strength; error was reported as the standard deviation of these means.

To determine the down-channel velocity (perpendicular to the field) the time and x-location of the particle when it crossed the channel centerline (Fig. S2) were collected. The down-channel velocity (Fig. S2) was calculated by linear regression on this data; the reported error represents the 95% confidence interval of the regression coefficient. For multiple measurements at the same field strength, normalized cross-channel velocities u / D were averaged and the error reported as the standard deviation. Where only single measurements were available, error is reported as the mean of the (relative) standard deviations of those values which had multiple values; this provides a more accurate representation of uncertainty (*i.e.*, a larger uncertainty) than the standard deviation of a single measurement.

3. Construction of barriers for the particle separator

The general method for constructing particle barriers in complex geometries follows three rules as reported in the main text: (*i*) a particle moves along field lines until it contacts a surface, (*ii*) a particle rolls along inclined barrier surfaces, and (*iii*) the particle reverses direction when it contacts an electrode surface. Here, we describe in detail the process used to construct the barriers for the particle separator in Fig. 3 of the main text and note several useful comments regarding barrier construction in general.

The curved geometry of the separator (Fig. 3a) was chosen to facilitate the injection of liquid gallium into PDMS channels to form the electrodes. Sharp electrode corners are generally difficult to fill without forcing the liquid gallium through the spaces between the dielectric barriers and into the central channels. Turn radii of about 100 μm or more are preferred; the radius of curvature used for the particle separator electrodes was 350 μm. The choice of electrode polarity was dictated by the desired operation, namely that the particles were to enter from the left channel and exit through the bottom right channel.

Having chosen the geometry and polarity of the electrodes, we used finite element analysis (COMSOL) to calculate the electric field lines (Fig. S3a). As noted in the text, one advantage of our ratchet technique is that barriers do not substantially alter the electric field because the dielectric constant of the teeth (PDMS, $\varepsilon \approx 2.3$) is similar to that of the dielectric fluid (mineral oil, $\varepsilon = 2.5$). Therefore, the design process is sequential rather than iterative, and the electric field need only be calculated once.

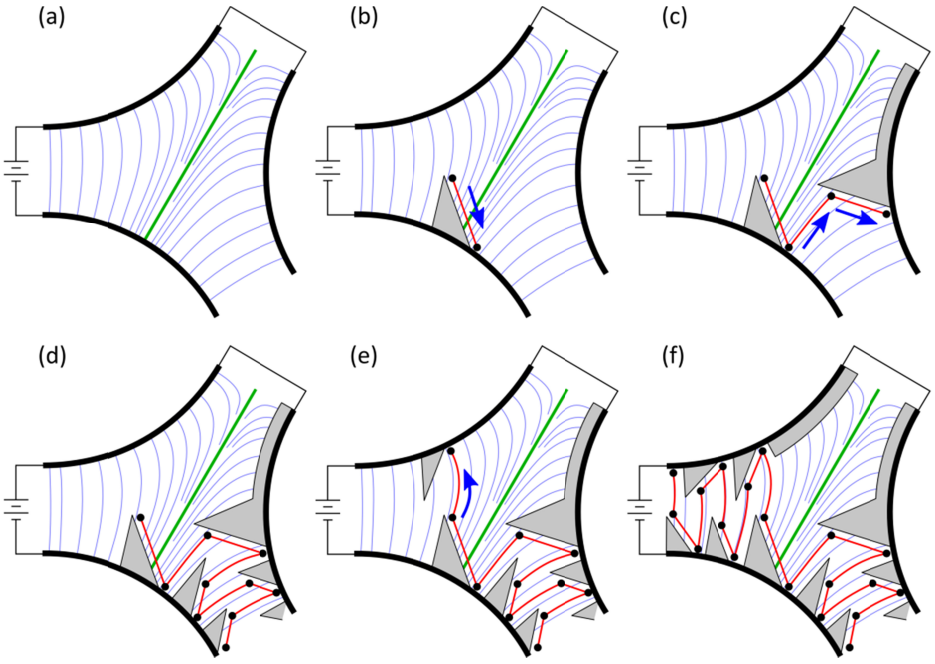

Fig. S3. *Barrier construction for the particle separator.* **(a)** Field lines were calculated by finite element modeling; the green line denotes the line of symmetry; the desired functionality is to direct particles from the left inlet to the bottom-right outlet. **(b)** A barrier is added to force the particle to cross the symmetry line in the direction noted by the blue arrow. **(c)** An additional barrier directs the motion of the particle towards the outlet. **(d)** The remaining outlet teeth are added in accordance with the rules presented in the text. **(e)** The process is repeated in reverse for adding teeth to the inlet stream; note that the particle will follow the curvature of the field line (rule (*i*)). **(f)** All teeth positioned to direct particle motion from the inlet on the left to the outlet on the lower-right.

The line of field symmetry denoted by the green line in Fig. S3a is the starting point for designing the teeth, because it represents a dividing line for particle oscillations between different electrodes. In the absence of the dielectric barriers, a particle initially located at any point on the left of the symmetry line will remain there indefinitely despite any electrophoretic

(or dielectrophoretic) motion; similarly, any particle on the right will remain on the right. Therefore, we require a barrier that will force the particle to cross the centerline. In designing the particle separator, we begin by positioning this key barrier across the centerline (Fig. S3b). According to design rule (*ii*), the particle will roll along the barrier in the direction denoted by the blue arrow until it contacts the lower electrode whereupon it will reverse direction (rule (*iii*)) and travel along whatever field line it currently resides upon (rule (*i*)). Importantly, the angle between the surface of the tooth and the field line at its surface should be ~45 °; smaller angles (*i.e.,* "sharper" teeth) are acceptable but may be difficult to fabricate via photolithography while larger angles may inhibit particle motion altogether. A new barrier is placed to direct this motion towards the outlet (Fig. S3c); this process of tracing field lines and sketching barriers is repeated as necessary to transport the particle out the lower-right channel (Fig. S3d). Note that the separation between teeth on the electrode surface and the distance which the tooth extends into the channel are both adjustable; generally, teeth spacing should be no more than 50 μm to avoid bulging or failure during electrode injection and the teeth should extend into the channel ~1/3 L.

With the outlet teeth in place, a similar process is used in reverse to position inlet teeth (Fig. S3e). Rule (*i*) is emphasized here because the curvature of the field line is significant; the path of the particle is traced in reverse and barriers are added until all teeth have been included (Fig. S3f). Note that additional smooth barriers have been included to form the outlet channel: the particle will not contact these surfaces but a barrier is necessary to contain and direct the liquid gallium when it is injected.

4. Down-channel velocity reduction

When a particle contacts a tooth in a ratcheted channel, it has been experimentally observed to translate and roll along the surface of the tooth (Fig. S4a and accompanying movie). The goal of this Section is to determine if this rolling and translation is consistent with the well-established hydrodynamic effects of particle movement near a stationary plane wall in an otherwise quiescent fluid. By extension, if the motion along the tooth can be explained in this manner, so too should the observed ratio of the down-channel to the cross-channel velocity. The geometry is sketched in Fig. S4b: a sphere of radius a subject to an electrostatic force F_{es} in the negative z-direction translates along an inclined plane with velocity u in the direction parallel to the surface.

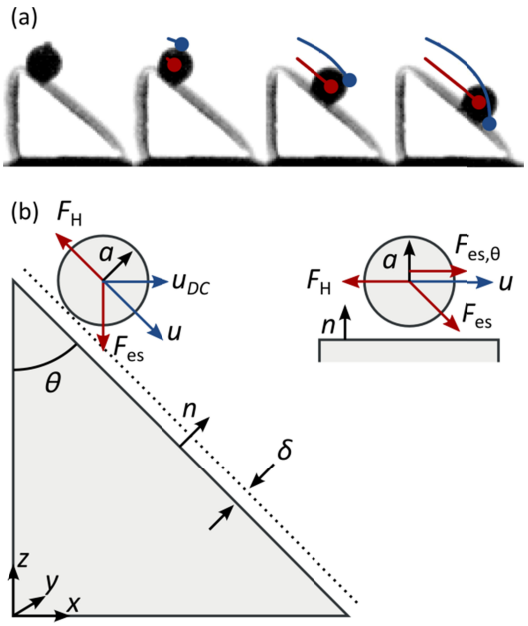

Fig. S4. *Translation and rotation.* **(a)** Experimental observation of translation and rotation of a 21 μm particle (E_o = 5.7 V/μm). The red marker and line trace the location of the sphere; the blue marker and line trace the location of a surface irregularity which is assumed not to interfere with the overall motion. **(b)** Tooth

and sphere geometry. The velocity u of the sphere along the surface of the tooth was determined from the images in (a) to be 0.014 m/s; the rotational velocity ω (not shown in figure) was similarly calculated to be 710 rad/s.

From Goldman[4] and Malysa[5], the translational and angular velocities, u and ω, of a torque-free sphere translating and rolling near a wall are given by

$$\mathbf{u} = -\frac{t^r F_{es} \cos\theta}{6\pi\eta a\left(t^r f^t - t^t f^r\right)}\left(\sin\theta \mathbf{e}_x - \cos\theta \mathbf{e}_z\right) \tag{S0}$$

$$\boldsymbol{\omega} = -\frac{t^t F_{es} \cos\theta}{6\pi\eta a^2\left(t^r f^t - t^t f^r\right)}\mathbf{e}_y \tag{S0}$$

where $-F_{es}\cos\theta$ is the component of the electrostatic force directed parallel to the surface, $\mathbf{e}_i$ is the unit vector in the i-direction, and t^r, t^t, f^r, and f^t are dimensionless drag coefficients. In the limit of small surface separations ($\delta / a << 1$), these coefficients are well approximated as

$$f^t = \frac{8}{15}\ln\left(\frac{\delta}{a}\right) - 0.9588, \quad t^t = -\frac{1}{10}\ln\left(\frac{\delta}{a}\right) - 0.1895 \tag{S0}$$

$$f^r = -\frac{2}{15}\ln\left(\frac{\delta}{a}\right) - 0.2526, \quad t^r = \frac{2}{5}\ln\left(\frac{\delta}{a}\right) - 0.3817 \tag{S0}$$

By contrast, when the particle moves across the channel, its translational velocity can be approximated as that of a sphere through an unbounded fluid,

$$\mathbf{u}_o = -\frac{F_{es}}{6\pi\eta a}\mathbf{e}_z \tag{S0}$$

The ratio of this cross-channel velocity u_o to the down-channel velocity u_x given by equation (S0) is therefore estimated to be

$$\left|\frac{u_o}{u_x}\right| = \left|\frac{t^r f^t - t^t f^r}{t^r \cos\theta \sin\theta}\right| \qquad \text{(S0)}$$

This ratio is plotted below as a function of the surface separation δ / a for the experimental barrier angle of $\theta = 45^o$. Experimentally, this ratio is estimated to be ~10. This implies a surface separation of several nanometers, which is physically reasonable.

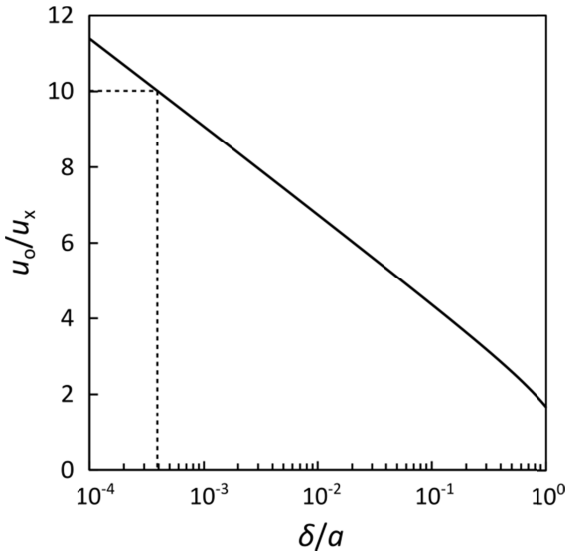

Fig. S5. Ratio of the cross-channel velocity to the down-channel velocity as a function of dimensionless surface separation as calculated by equation (S0).

Interestingly, the angular velocity of the particle moving along the dielectric barrier is larger than that expected by low-Reynolds number hydrodynamics but smaller than that of pure rolling. This is clearly illustrated by comparing the dimensionless "slip factor" $a\omega / u$ between experiment and theory (Fig. S6). For the experimental system shown in Fig. S4a, u_{exp} = 0.014

m/s and ω_{exp} = 710 rad/s such that $a\omega/u = 0.54$. For pure rolling motion – that is, no slip between the contacting surfaces – this quantity should be identically one, $a\omega/u = 1$. By contrast, the hydrodynamic model summarized in equations (S0) and (S0) predicts that

$$\frac{a\omega}{u} = -\frac{t^t}{t^r} \qquad \text{(S0)}$$

This quantity depends on the surface separation δ as illustrated in Figure S6 but is generally less than 0.25. The discrepancy between experiment and the hydrodynamic model is likely due to mechanical surface roughness, which is unaccounted for in the model and undoubtedly important at small surface separations (several nm).

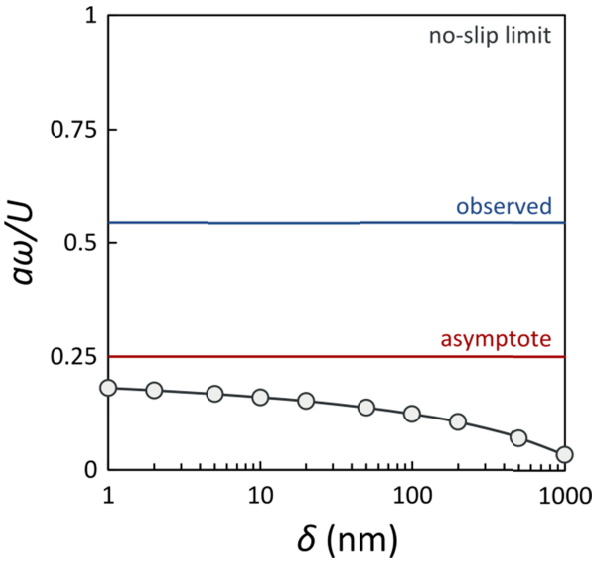

Fig. S6. Dimensionless slip factor $a\omega/u$ as a function of surface separation distance δ. The grey line and points represent the hydrodynamic model [equation (S0)] which asymptotically approaches 0.25 as $\delta \to 0$. In the limit of perfect rolling (no-slip), $a\omega/u = 1$. The experimentally observed value of 0.54 lies in between these limiting cases.

5. Supporting Movies

Experimental details for each of the movies accompanying the main text are as follows.

1. **Rolling motion**
    a. Acquisition = 18006 fps
    b. Playback = 30 fps **(600 times slowed)**
    c. Particle diameter = 21 μm
    d. Electrode spacing = 140 μm
    e. Voltage = -800 V
    f. Description: A 21 μm particle demonstrates the rolling motion of a particle on the surface of dielectric barriers (teeth). Note the small protrusion on the surface of the sphere.

2. **Ratcheting behavior of Fig. 1d**
    a. Acquisition = 6000 fps
    b. Playback = 50 fps **(120 times slowed)**
    c. Particle diameter = 16 μm
    d. Electrode spacing = 150 μm
    e. Voltage = 600 V
    f. Description: A 16 μm particle demonstrates the standard ratchet mechanism.

3. **Transport of dissolved species**
    a. Acquisition = 17000 fps
    b. Playback = 50 fps **(340 times slowed)**
    c. Particle diameter = 36 μm
    d. Electrode spacing = 140 μm
    e. Voltage = 800 V
    f. Description: A porous agarose bead was loaded with aqueous red dye (which appears black in monochromatic movies). The bead ratchets in the same manner as Ag-coated hollow glass spheres.

4. **Upstream rectification of Fig. 2b (including PS particles)**
    a. Acquisition = 14000 fps
    b. Playback = 500 fps **(28 times slowed)**
    c. Particle diameter = 12 μm
    d. Electrode spacing = 140 μm
    e. Voltage = 1200 V
    f. Description: A silver-coated hollow glass sphere moves upstream against mineral oil flowing from right to left at 50 μL/hr. The centerline velocity of mineral oil was about 1 mm/s as determined by the 1 μm polystyrene tracer particle (white dot in movie).

5. **Particle separator**
    a. Acquisition = 10000 fps
    b. Playback = 30 fps **(333 times slowed)**
    c. Particle diameter = 20 μm
    d. Electrode spacing = 140 μm (closest)
    e. Voltage = 1200 V
    f. Description: A silver-coated hollow glass sphere enters from the left and is split from a flow of mineral oil (200 uL/hr, ~10 mm/s outlet flow velocity).

6. **Multiple particles**
    a. Acquisition = 17000 fps
    b. Playback = 50 fps (340 times slowed)
    c. Particle diameter = varies
    d. Electrode spacing = 140 μm
    e. Voltage = 800 V
    f. Description: A large particle (D ~ 28 μm) overtakes a smaller particle (D ~ 13 μm) in a ratcheted channel.

References

1. Y. N. Xia and G. M. Whitesides, *Annu. Rev. Mater. Sci.*, 1998, **28**, 153-184.
2. J.-H. So and M. D. Dickey, *Lab Chip*, 2011, **11**, 905-911.
3. D. Blair and E. Dufresne, The Matlab Particle Tracking Code Repository, http://physics.georgetown.edu/matlab/, Accessed January 1, 2010.
4. A. J. Goldman, R. G. Cox and H. Brenner, *Chem. Eng. Sci.*, 1967, **22**, 637-651.
5. K. Małysa and T. G. M. van de Ven, *International Journal of Multiphase Flow*, 1986, **12**, 459-468.
6. H. Brenner, *Chem. Eng. Sci.*, 1961, **16**, 242-251.